

Accuracy Enhancing Interface Treatment Algorithm: the Back and Forth Error Compensation and Correction method

Wenbin Dong*

Yingjie Liu†

Hansong Tang‡

May 24, 2022

Abstract

The accuracy of information transmission while solving domain decomposed problems is crucial to smooth transition of a solution around the interface/overlapping region. This paper describes a systematical study on an accuracy enhancing interface treatment algorithm based on the back and forth error compensation and correction method (BFEC). By repetitively employing a low order interpolation technique (normally local 2nd order) 3 times, this algorithm achieves local 3rd order accuracy. Analytical derivations for 1D & 2D cases are made, and the “super convergence” phenomenon (4th order accuracy) is found for specific positioning of the donor and target grids. A set of numerical experiments based on various relative displacements, relative rotations, mesh ratios, and meshes with perturbation have been tested, and the results match the derivations. Different interface treatments are compared with 3D examples: corner flow and cavity flow. The component convergence rate analysis shows that the BFEC method positively affects the accuracy of solutions.

1 Introduction

It is important to have accurate numerical treatments at grid or model interfaces and for those of the algorithms to be coupled in subdomains. Commonly the algorithms within each subdomain are 2nd order accurate, or, locally 3rd order accurate, while interface algorithms are at most locally 2nd order accurate, e.g., in flow simulations [4, 18, 20]. Therefore, it is important to develop locally 3rd order accurate methods which are easy to use on nonuniform grids for interface algorithms, so that the numerical accuracy will be uniformly 2nd order in the whole computational domain.

*wdong000@citymail.cuny.edu, Civil Engineering Department, City College of New York, City University of New York, New York, NY 10031, USA.

†yingjie@math.gatech.edu, School of Mathematics, Georgia Institute of Technology, Atlanta, GA 30332.

‡htang@ccny.cuny.edu, Civil Engineering Department, City College of New York, City University of New York, New York, NY 10031, USA.

Key words: BFEC, interpolation accuracy, super-convergence, ratio of grid spacing, rotation of grid, MFBI

MSC: 65M06, 65M08, 65M55

Declarations: **Funding.** This work is supported in part by National Science Foundation (DMS # 1622459 and 1622453).

Conflicts of interest/Competing interests. There is no conflicts of interest. **Availability of data and material.** Data is available within the article. **Code availability.** The code is available upon request.

Interpolation is a key step for interface treatments, and there exist many high-order interpolation methods, such as Lagrangian methods and spline methods, e.g., [6, 10]. However, in general, a high-order interpolation needs 1) more grid nodes whose values are interpolated and 2) solving a linear system to determine interpolation coefficients (in particular for irregular grids [3]). When the spatial dimension gets higher, both 1) and 2) are expensive for computation, and they are often difficult to implement in practical computation, e.g., in interpolation between irregular grids. To achieve 3rd order accuracy locally at interfaces requires looking beyond adjacent grid points by existing methods.

A high order conservative interpolation method for moving meshes was introduced in [21] which proposed a fictitious advection equation representing the mesh movement and solved it with a high order finite volume scheme to achieve the conservative interpolation. In this research, we utilize the BFECC method [8] to achieve 3rd order accuracy locally by calling a local linear interpolation algorithm 3 times. For example, for an advection equation (u is a scalar, and \mathbf{V} is a vector)

$$u_t + \mathbf{V} \cdot \nabla u = 0, \quad (1)$$

with the 1st order CIR scheme [7] as the underlying scheme, BFECC provides a procedure, as outlined in Sec.2, to enhance the accuracy to 2nd order accurate, thus improving the local order of accuracy to 3rd order. The advantage of the BFECC method is that it does not increase the complexity of the simple underlying scheme, but just repeat the computation using the same scheme for two extra times.

When there is no advection, or, $\mathbf{V} = 0$ in Eq. (1), the grid at an old-time level is the original grid and the grid at a new-time level is the grid to be interpolated to. Then, the BFECC method becomes an interpolation method that achieves local 3rd order accuracy if a local linear interpolation is used in the underlying scheme. In comparison with standard higher-order accurate interpolation methods, BFECC keeps the simplicity (and three times the complexity) of the underlying linear interpolation, and it can be implemented to existing computer codes by recycling an existing 2nd order interface algorithms. There has been research work on BFECC for quadtree-octree mesh refinement, e.g., in [1, 2] for fluid simulations, [22] for transport equations, [5] for locally refined Lattice Boltzmann method, and for interpolation between equilateral triangular grids [13]. The interpolation can also be viewed as solving Eq. (1) on the fixed old grid by a numerical scheme with \mathbf{V} describing the mesh movement between the old and new grids [21], and the case with the numerical scheme being BFECC was mentioned in [9].

In this paper, the BFECC method is analyzed and experimented with regard to its implementation, effectiveness, and limitations as a systematical study on its application to interpolation on structured meshes. For a comparison, 2nd order interpolation and MFBI (mass-flux based interpolation) are also discussed [17]. The rest of the paper is organized as follows: in Section 2, we introduce the algorithm of BFECC and discuss its accuracy as well as some other concerns in 1D, 2D & 3D cases. Section 3 provides the numerical simulation results for cavity flow and corner flow. Then we finish this paper in Section 4 with conclusions.

2 BFECC Interpolation

2.1 Algorithm and Accuracy

Considering equation (1) in d space dimensions as an example, Let L be a numerical scheme for (1) which advances the numerical solution at the time level t_n , U^n forward to the next time level t_{n+1} , i.e., $U^{n+1} = L\{U^n\}$. The BFECC method [8] can be described as follows.

1. **Forward advection:**

$$\tilde{U}^{n+1} = L\{U^n\}.$$

2. **Backward advection:**

$$\tilde{U}^n = L^*\{\tilde{U}^{n+1}\},$$

where L^* is L applied to the time reversed equation of (1), $u_t - \mathbf{V} \cdot \nabla u = 0$.

3. **Error compensation:**

$$\hat{U}^n = U^n + \frac{U^n - \tilde{U}^n}{2}.$$

4. **Forward advection:**

$$U^{n+1} = L\{\hat{U}^n\}.$$

Assume scheme L is a linear scheme on a rectangular grid \mathcal{G}_1 with mesh sizes $\Delta x_1 = \Delta x_2 = \dots = \Delta x_d \equiv \Delta x$, and the Fourier symbols of L and L^* , ρ_L and ρ_{L^*} respectively, satisfy $\rho_{L^*} = \overline{\rho_L}$ (the complex conjugate of ρ_L), then we have the following theorem ([9], Theorem 4).

Theorem 1 Suppose scheme L is accurate of order r for equation (1) with constant coefficients, where r is an odd positive integer, then after applying BFECC to scheme L , it is accurate of order $r + 1$.

Let \mathcal{G}_2 be another rectangular grid generated by shifting grid \mathcal{G}_1 along an arbitrary constant vector \mathbf{w} , $|\mathbf{w}| = O(\Delta x)$. Let f be a sufficiently smooth function defined at grid points of grid \mathcal{G}_1 , then interpolating the value of f from grid points of \mathcal{G}_1 to grid points of \mathcal{G}_2 can be performed as follows analogous to the above BFECC method.

1. **Forward interpolation:**

Denote the value of f at grid point \mathbf{i} as $f_{\mathbf{i}}$, for every grid point \mathbf{i} of \mathcal{G}_1 . Use local linear interpolation (e.g., bilinear interpolation in 2D, trilinear interpolation in 3D, etc) to interpolate the value of f from grid points of \mathcal{G}_1 to every grid point of \mathcal{G}_2 .

2. **Backward interpolation:**

Use local linear interpolation to interpolate from grid points of \mathcal{G}_2 to grid point \mathbf{i} of \mathcal{G}_1 to obtain $\tilde{f}_{\mathbf{i}}$, for every grid point \mathbf{i} of \mathcal{G}_1 .

3. **Error compensation:**

Define $\hat{f}_{\mathbf{i}} = f_{\mathbf{i}} + \frac{1}{2}(f_{\mathbf{i}} - \tilde{f}_{\mathbf{i}})$, for every grid point \mathbf{i} of \mathcal{G}_1 .

4. **Forward interpolation:**

Use local linear interpolation to interpolate the values $\{\hat{f}_{\mathbf{i}}\}$ from grid points of \mathcal{G}_1 to every grid point of \mathcal{G}_2 .

This interpolation method will be referred to as **BFECC interpolation** for the rest of the paper. Note that the above BFECC interpolation can be applied to interpolation between two irregular or unstructured meshes as long as the local linear interpolation is properly defined, e.g., as local linear least squares. Now we are going to identify BFECC interpolation with solving an advection equation with BFECC following [21]. Replace \mathbf{V} with $-\mathbf{w}/\Delta x$ in equation (1) and let the initial value of this equation

be f . Then solve equation (1) for just one time step with the time step size $\Delta t = \Delta x$ by the scheme formed by BFECC applied to the CIR scheme [7] (with local linear interpolation). It is easy to see that the numerical solution at grid point \mathbf{i} and at the time Δt is the interpolated value at grid point $\mathbf{i} + \mathbf{w}$ of grid \mathcal{G}_2 obtained by the above BFECC interpolation. BFECC applied to the CIR scheme is 2nd order accurate according to Theorem 1, or equivalently is 3rd order accurate for just one time step. We have proved the following theorem.

Theorem 2 *BFECC interpolation from a uniform rectangular grid in k dimensions (for any positive integer k , with mesh sizes $\Delta x_1 = \Delta x_2 = \dots = \Delta x_k$) to a shifted grid along any vector is 3rd order accurate.*

Since the interpolation between two grids is equivalent to solving an advection equation for one time step by a numerical scheme, we have also tested another simple scheme, the modified MacCormack scheme [15] which uses only two advection steps. Note that Theorem 2 can be generalized when the local linear interpolation is replaced by local interpolation with a $(2k + 1)$ -th degree polynomial, $k = 1, 2, 3, \dots$, and the corresponding order of BFECC interpolation becomes $2k + 3$.

2.2 Super-Convergence

Consider in one dimension the BFECC interpolation for a sufficiently smooth function $f(x)$, from f_i defined on the source grid to f_j on the target grid, as shown in Fig.1. Here the target grid is obtained by shifting the source grid (uniform with grid size Δx) to the right with a distance d . Let $\alpha = d/\Delta x$. The

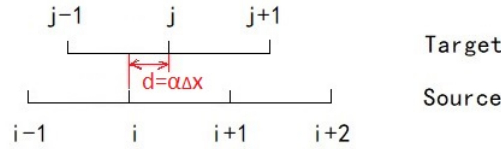


Figure 1: 1D grids for interpolation

function value at node j of the target grid is interpolated from its values in the source grid as follows:
Forward interpolation:

$$\begin{aligned}
 &\dots \\
 f_{j-1}^* &= \alpha f_i + (1 - \alpha) f_{i-1} \\
 f_j^* &= \alpha f_{i+1} + (1 - \alpha) f_i \\
 f_{j+1}^* &= \alpha f_{i+2} + (1 - \alpha) f_{i+1} \\
 &\dots
 \end{aligned} \tag{2}$$

Backward interpolation:

$$\begin{aligned}
 &\dots \\
 \tilde{f}_i &= \alpha f_{j-1}^* + (1 - \alpha) f_j^* \\
 \tilde{f}_{i+1} &= \alpha f_j^* + (1 - \alpha) f_{j+1}^* \\
 &\dots
 \end{aligned} \tag{3}$$

Error compensation:

$$\begin{aligned} & \dots \\ & \hat{f}_i = f_i + (f_i - \tilde{f}_i)/2 \\ & \hat{f}_{i+1} = f_{i+1} + (f_{i+1} - \tilde{f}_{i+1})/2 \\ & \dots \end{aligned} \tag{4}$$

Forward interpolation:

$$\begin{aligned} & \dots \\ & f_j^{new} = \alpha \hat{f}_{i+1} + (1 - \alpha) \hat{f}_i \\ & \dots \end{aligned} \tag{5}$$

Here f_j^{new} is the interpolated value at node j by BFECC interpolation. Using Taylor expansions (at node j), a straightforward derivation shows that

$$f_j^{new} = f_j + \frac{\alpha(\alpha - 1)[(8\alpha - 4)\Delta x^3(f_{xxx})_j - 9\alpha(\alpha - 1)\Delta x^4(f_{xxxx})_j]}{24} + \mathcal{O}(\Delta x^4). \tag{6}$$

Formula (6) is derived using a program of symbolic calculation in the software of 'Mathematica' (version: 11.3.0). The code is attached in Appendix A. This implies that the error of the BFECC interpolation is 3rd order accurate. **And if $\alpha = \frac{1}{2}$, i.e., the interpolation point is located at the centroid of a cell of the grid, the term with Δx^3 on the right hand side disappears, then the interpolation has 4th order accuracy, a “super-convergence” phenomenon.** As a comparison, if only the forward interpolation step is applied, then

$$f_j^* = f_j + \frac{\alpha(1 - \alpha)\Delta x^2(f_{xx})_j}{2} + \mathcal{O}(\Delta x^3), \tag{7}$$

which is 2nd order accurate.

Now consider a 2D rectangular grid $\mathcal{G}_1 = \{(i\Delta x, j\Delta y) : \text{for any integers } i, j\}$. Let \mathcal{G}_2 be the grid generated by shifting \mathcal{G}_1 along the vector $(\alpha\Delta x, \beta\Delta y)$, $0 \leq \alpha, \beta \leq 1$, see Fig.2. Consider the BFECC interpolation from \mathcal{G}_1 to \mathcal{G}_2 for a sufficiently smooth function $f(x, y)$. Using 2D Taylor expansions around an interpolation point $(r, s) = (i + \alpha, j + \beta)$, we obtain the interpolation accuracy similar to the 1D case (6):

$$\begin{aligned} f_{(r,s)}^{new} = f_{(r,s)} & + \frac{(\alpha - 3\alpha^2 + 2\alpha^3)\Delta x^3(f_{xxx})_{(r,s)} + (\beta - 3\beta^2 + 2\beta^3)\Delta y^3(f_{yyy})_{(r,s)}}{6} \\ & + \mathcal{O}(\Delta x^4 + \Delta y^4), \end{aligned} \tag{8}$$

where $f_{(r,s)}^{new}$ is the interpolated value at shifted grid point (r, s) which is 3rd order accurate. **In particular, when $\alpha = \beta = \frac{1}{2}$, $f_{(r,s)}^{new}$ is 4th order accurate.** The 'Mathematica' (version: 11.3.0) code to derive Formula (8) is attached in Appendix B. As a comparison, bi-linear interpolation at (r, s) has

$$\begin{aligned} f_{(r,s)}^* = f_{(r,s)} & + \frac{1}{2}(\alpha - \alpha^2)\Delta x^2(f_{xx})_{(r,s)} \\ & + \frac{1}{2}(\beta - \beta^2)\Delta y^2(f_{yy})_{(r,s)} + \mathcal{O}(\Delta x^3 + \Delta y^3), \end{aligned} \tag{9}$$

which is only 2nd order accurate. We summarize these results in the following theorem.

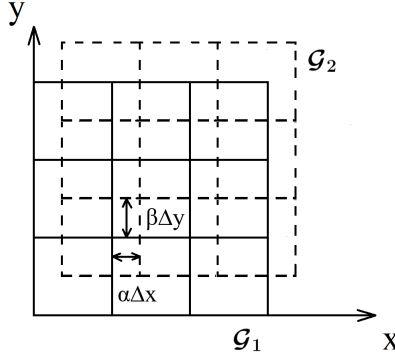


Figure 2: 2D grids for interpolation

Theorem 3 *BFECC interpolation from a uniform rectangular grid in 1D or 2D (with mesh sizes Δx and Δy) to a shifted grid along any vector is 3rd order accurate. In particular, if the shifted grid points are located at centroids of the original grid cells, then BFECC interpolation is 4th order accurate.*

Numerical experiments show that Theorem 3 holds in 3D. We have the following conjecture.

Conjecture 4 *BFECC interpolation from a uniform rectangular grid in d dimensions (for any positive integer d , with mesh sizes $\Delta x_1, \Delta x_2, \dots, \Delta x_d$) to a shifted grid along any vector is 3rd order accurate. In particular, if the shifted grid points are located at centroids of the original grid cells, then BFECC interpolation is 4th order accurate.*

2.3 Numerical Tests

In order to verify the above discussion, numerical tests have been conducted. To obtain the order of convergence rate using linear interpolation and BFECC interpolation (based on the linear interpolation.), four sets of grids are used with grid sizes $\Delta x = 0.05, 0.025, 0.0125$ & 0.00625 . The computed orders of accuracy against a 1D exact function are listed in Table 1. The 2D convergence results can be found in Table 2. When interpolation points are located at centroids of grid cells, BFECC interpolation gives 4th order accuracy in 2D, see Table 3. In Table 4, BFECC interpolation is compared to the interpolation based on the modified MacCormack scheme (the interpolation is performed by solving an advection equation with the scheme for one time step, see the discussion near the end of Sec. 2.1.) While both methods have 3rd order accuracy, BFECC interpolation errors tend to be several times smaller. Similar comparison tests are conducted with different interpolated functions in Tables 5 and 6, and with interpolation points located at centroids of grid cells in Table 7. Note that BFECC interpolation has 4th order accuracy at centroids while the interpolation based on the modified MacCormack scheme doesn't have "super-convergence" there. Bilinear interpolation is replaced by linear least squares method in some examples as the underlying interpolation method which doesn't change the order of convergence. Least squares interpolation is suitable for irregular meshes, see e.g., [3, 12] for high order least squares interpolation for WENO reconstruction on unstructured meshes and [23] for using linear least squares on irregular meshes to construct an underlying scheme of BFECC to solve the Maxwell's equations. We

will extend BFECC interpolation to non uniform grids next and linear least squares interpolation will be used as the underlying interpolation method for BFECC. When the interpolation point is at the centroid of a rectangle, both bilinear interpolation and linear least squares are simple average of function values at vertices of the rectangle.

1D, Grid Shift $\mathbf{w} = 0.25\Delta x$				
	Linear Interpolation		BFECC	
Δx	error	order	error	order
0.05	7.19E-4		5.80E-5	
0.025	1.67E-4	2.11	7.26E-6	3.00
0.0125	4.00E-5	2.06	9.10E-7	3.00
0.00625	9.81E-6	2.03	1.14E-7	3.00

Table 1: Accuracy of linear interpolation and BFECC interpolation in 1D. Interpolated function: $f(x) = \sin(\pi * x)$.

2D, Grid Shift $\mathbf{w} = (0.25\Delta x, 0.25\Delta y)$, $\Delta x = \Delta y$				
	Bilinear Interpolation		BFECC	
Δx	error	order	error	order
0.05	2.26E-3		8.40E-5	
0.025	5.24E-4	2.11	1.08E-5	2.95
0.0125	1.27E-4	2.05	1.33E-6	3.03
0.00625	3.11E-5	2.03	1.18E-7	2.99

Table 2: Accuracy of bilinear and BFECC interpolations in 2D. Interpolated function: $f(x, y) = \sin(\pi * (x + 2y))$.

2D, Grid Shift $\mathbf{w} = (0.5\Delta x, 0.5\Delta y)$, $\Delta x = \Delta y$				
	Bilinear Interpolation		BFECC	
Δx	error	order	error	order
0.05	1.93E-3		2.01E-4	
0.025	4.57E-4	2.08	1.27E-5	3.98
0.0125	1.12E-4	2.03	7.93E-7	4.01
0.00625	2.76E-5	2.01	4.98E-8	3.99

Table 3: Super-convergence of BFECC interpolation based on bilinear interpolation in 2D. Interpolated function: $f(x, y) = \sin(\pi * (x + 2y))$.

2D, Grid Shift $\mathbf{w} = (0.25\Delta x, 0.25\Delta y)$, $\Delta x = \Delta y$						
	Linear least squares		BFECC		Maccormack	
Δx	error	order	error	order	error	order
0.05	7.63E-4		5.85E-5		1.66E-4	
0.025	1.76E-4	2.11	7.31E-6	3.00	2.08E-5	2.99
0.0125	4.24E-5	2.06	9.16E-7	3.00	2.61E-6	3.00
0.00625	1.04E-5	2.03	1.15E-7	3.00	3.27E-7	3.00

Table 4: Accuracy of linear least squares, and BFECC and Maccormack interpolation methods based on it in 2D. Interpolated function: $f(x, y) = \sin(\pi * (x + 0.2y))$.

2D, Grid Shift $\mathbf{w} = (0.25\Delta x, 0.25\Delta y)$, $\Delta x = \Delta y$						
	Linear least squares		BFECC		Maccormack	
Δx	error	order	error	order	error	order
0.05	1.53E-4		1.18E-5		3.38E-5	
0.025	3.51E-5	2.12	1.48E-6	3.00	4.22E-6	3.00
0.0125	8.42E-6	2.06	1.85E-7	3.00	5.27E-7	3.00
0.00625	2.06E-6	2.03	2.31E-8	3.00	6.59E-8	3.00

Table 5: Accuracy of linear least squares, and BFECC and Maccormack interpolation methods based on it in 2D. Interpolated function: $f(x, y) = (x + 0.2y)^3$.

2D, Grid Shift $\mathbf{w} = (0.25\Delta x, 0.25\Delta y)$, $\Delta x = \Delta y$						
	Linear least squares		BFECC		Maccormack	
Δx	error	order	error	order	error	order
0.05	2.52E-4		1.93E-6		5.71E-6	
0.025	6.22E-5	2.02	2.45E-7	2.98	7.11E-7	3.01
0.0125	1.55E-5	2.01	3.08E-8	2.99	8.87E-8	3.00
0.00625	3.85E-6	2.00	3.86E-9	2.99	1.11E-8	3.00

Table 6: Accuracy of linear least squares, and BFECC and Maccormack interpolation methods based on it in 2D. Interpolated function: $f(x, y) = \exp(x + 0.2y)$.

2D, Grid Shift $\mathbf{w} = (0.5\Delta x, 0.5\Delta y)$, $\Delta x = \Delta y$						
	Linear least squares		BFECC		Maccormack	
$\Delta x = \Delta y$	error	order	error	order	error	order
0.05	3.38E-4		1.65E-7		9.95E-6	
0.025	8.32E-5	2.02	1.01E-8	4.02	1.24E-6	3.01
0.0125	2.06E-5	2.01	6.29E-10	4.01	1.54E-7	3.00
0.00625	5.14E-6	2.01	3.91E-11	4.01	1.92E-8	3.00

Table 7: Super-convergence study of linear least squares, and BFECC and Maccormack interpolation methods based on it in 2D. Interpolated function: $f(x, y) = \exp(x + 0.2y)$.

BFECC interpolation on 3D rectangular grids is also tested in Tables 8 and 9, with the underlying interpolation method being trilinear and linear least squares respectively. Again, “super-convergence” is found for BFECC interpolation if interpolation points are located at centroids of grid cells, see Table 10. We have also tested 3D uniform rectangular grids with $\Delta x \neq \Delta y \neq \Delta z$ and found Theorem 3 still true. These numerical tests are presented in Tables 11, 12 and 13.

3D, Grid Shift $\mathbf{w} = (0.25\Delta x, 0.25\Delta y, 0.25\Delta z)$, $\Delta x = \Delta y = \Delta z$				
	Trilinear Interpolation		BFECC	
Δx	error	order	error	order
0.05	2.28E-2		1.88E-3	
0.025	5.68E-3	2.00	2.06E-4	3.19
0.0125	1.41E-3	2.01	2.48E-5	3.05
0.00625	3.51E-4	2.01	3.08E-6	3.01

Table 8: Accuracy of trilinear and BFECC interpolation in 3D. Interpolated function: $f(x, y, z) = \sin(\pi * (x + 2y + 3z))$.

3D, Grid Shift $\mathbf{w} = (0.25\Delta x, 0.25\Delta y, 0.25\Delta z)$, $\Delta x = \Delta y = \Delta z$				
	Linear Least Squares		BFECC	
Δx	error	order	error	order
0.05	1.12E-2		1.03E-3	
0.025	2.73E-3	2.04	1.29E-4	2.99
0.0125	6.73E-3	2.02	1.64E-5	2.99
0.00625	1.67E-4	2.01	2.04E-6	2.99

Table 9: Accuracy of linear least squares and BFECC interpolation based on it in 3D. Interpolated function: $f(x, y, z) = \sin(\pi * (x + 2y + 3z))$.

3D, Grid Shift $\mathbf{w} = (0.5\Delta x, 0.5\Delta y, 0.5\Delta z)$, $\Delta x = \Delta y = \Delta z$				
	Trilinear Interpolation		BFECC	
Δx	error	order	error	order
0.05	3.02E-2		1.90E-3	
0.025	7.57E-3	2.13	1.22E-4	3.97
0.0125	1.88E-3	2.06	7.60E-6	4.00
0.00625	4.68E-4	2.03	4.74E-7	4.00

Table 10: Super-convergence of BFECC interpolation based on trilinear interpolation in 3D. Interpolated function: $f(x, y, z) = \sin(\pi * (x + 2y + 3z))$.

3D, Grid Shift $\mathbf{w} = (0.25\Delta x, 0.25\Delta y, 0.25\Delta z)$, $\Delta x : \Delta y : \Delta z = 1:0.9:1.2$				
	Trilinear Interpolation		BFECC	
Δx	error	order	error	order
0.05	2.85E-2		2.75E-3	
0.025	7.21E-3	1.99	2.97E-4	3.21
0.0125	1.80E-3	2.00	3.55E-5	3.06
0.00625	4.49E-4	2.00	4.39E-6	3.01

Table 11: Accuracy of trilinear and BFECC interpolation in 3D. Interpolated function: $f(x, y, z) = \sin(\pi * (x + 2y + 3z))$.

3D, Grid Shift $\mathbf{w} = (0.5\Delta x, 0.5\Delta y, 0.5\Delta z)$, $\Delta x : \Delta y : \Delta z = 1:0.9:1.2$				
	Trilinear Interpolation		BFECC	
Δx	error	order	error	order
0.05	3.77E-2		2.90E-3	
0.025	9.59E-3	1.97	1.89E-4	3.94
0.0125	2.40E-3	2.00	1.19E-5	3.99
0.00625	5.99E-4	2.00	7.44E-7	4.00

Table 12: Super-convergence of BFECC interpolation based on trilinear interpolation in 3D. Interpolated function: $f(x, y, z) = \sin(\pi * (x + 2y + 3z))$.

3D, Grid Shift $\mathbf{w} = (0.25\Delta x, 0.25\Delta y, 0.25\Delta z)$, $\Delta x : \Delta y : \Delta z = 1:0.9:1.2$				
	Linear Least Squares		BFECC	
Δx	error	order	error	order
0.05	1.59E-2		8.26E-4	
0.025	3.92E-3	2.02	8.86E-5	3.22
0.0125	9.73E-4	2.01	1.06E-5	3.06
0.00625	2.42E-4	2.01	1.32E-6	3.01

Table 13: Accuracy of linear least squares and BFECC interpolation in 3D. Interpolated function: $f(x, y, z) = \sin(\pi * (x + 2y + 3z))$.

2.4 Interpolation Between Grids of Different Spacing

BFECC interpolation can be implemented between two non-uniform grids with ease. We consider the interpolation accuracy when the BFECC interpolation is between two parallel rectangular grids of different spacing. A 3D numerical experiment is conducted as shown in Fig.3, in which BFECC interpolation (with the underlying trilinear interpolation) will be made from grid S to T with grid sizes $\sqrt{2} : 1$ respectively. The results are presented in Table 14. It is clear that, in comparison to trilinear interpolation, BFECC interpolation reduces its errors in general but makes no improvement of the convergence order.

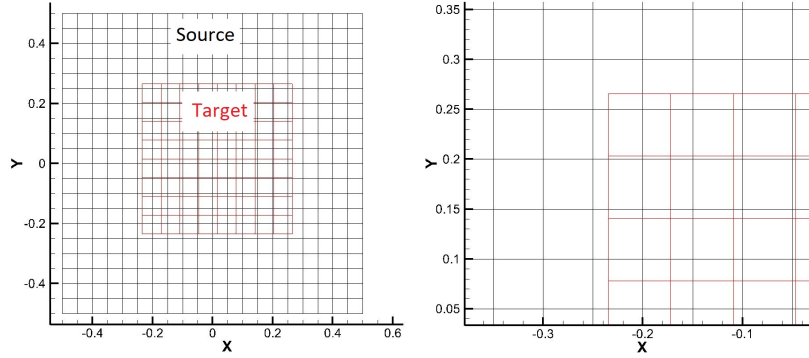


Figure 3: Grid size ratio of $\sqrt{2} : 1$.

3D, Grid spacing ratio of $\sqrt{2} : 1$				
Δx	Trilinear		BFECC	
	error	order	error	order
0.0625	5.21E-3		2.89E-3	
0.03125	1.21E-3	2.11	6.95E-4	2.05
0.015625	2.67E-4	2.18	1.74E-4	2.00
0.0078125	5.96E-5	2.16	4.24E-5	2.04

Table 14: Accuracy & order of trilinear and BFECC interpolation for 3D grids of size ratio $\sqrt{2} : 1$. Interpolated function: $f(x, y, z) = \sin(\pi * (x + 2y + 3z))$.

If the BFECC interpolation is from a coarse grid to a fine grid and the ratio of two grid spacing is far from 1:1, a remedy is to view the fine grid as the overlap of several subgrids so the ratio of the grid size of the coarse grid to that of a subgrid is close to 1:1. Fig. 4 shows an example which has 1:2 grid size ratio of a fine grid, the target grid, and a coarse grid, the source grid, and the splitting of the fine grid into two subgrids. Then the BFECC interpolation can be applied to the interpolation between the coarse grid (the source grid) and each of the subgrids to achieve 3rd order accuracy. An numerical example of the 3D BFECC interpolation between the coarse grid and a subgrid in the fine grid similar to Fig.4.

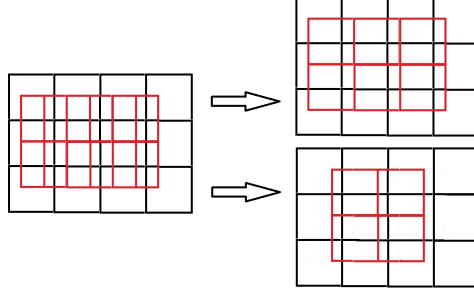


Figure 4: Fine grid is divided into 2 coarse grids to meet the 1:1 ratio.

2.5 Smoothly Perturbed Rectangular Grids

BFECC interpolation from a rectangular grid to a shifted and smoothly perturbed grid still has 3rd order accuracy. For example, consider the grid defined by (10) which is the shift and smooth perturbation from a rectangular grid ((10) without the terms containing "sin" functions), see Fig. 5.

$$\begin{aligned} x(i, j, k) &= (i - 1)\Delta x - 0.5L_x + 0.1\Delta x \sin(\pi * ((i - 1)\Delta x - 0.5L_x)), \\ y(i, j, k) &= (j - 1)\Delta y - 0.5L_y + 0.1\Delta y \sin(\pi * ((j - 1)\Delta y - 0.5L_y)), \\ z(i, j, k) &= (k - 1)\Delta z - 0.5L_z + 0.1\Delta z \sin(\pi * ((k - 1)\Delta z - 0.5L_z)), \end{aligned} \quad (10)$$

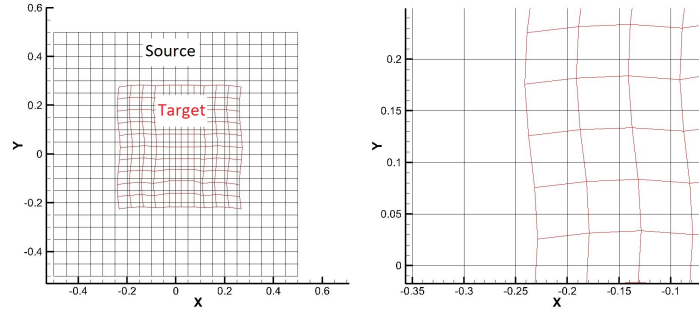


Figure 5: The target grid is smoothly perturbed and shifted from the source grid.

where ' L_x ', ' L_y ', and ' L_z ' are lengths of the domain in x, y and z directions. The target grid (the former one) deviates up to 20% from the the source grid (the latter one). The BFECC interpolation of the function $f = \sin(x + 2y + z^2)$ from the source grid ($\Delta x = \Delta y = \Delta z$) to the target grid is shown in Table 15. With the non uniform deformation from the source grid, the order of accuracy of BFECC interpolation still gets around 3rd order.

2.6 Rotated Rectangular Grids

When the grid is rotated, the BFECC interpolation from the original grid to it tends to improve the accuracy of the underlying interpolation method, but no longer improves the order of convergence. Here

From rectangular grid with $\Delta x = \Delta y = \Delta z$ to smoothly perturbed grid				
Grid Shift $w = (0.25\Delta x, 0.25\Delta y, 0.25\Delta z)$				
	Trilinear		BFECC	
Δx	error	order	error	order
0.0125	6.26E-5		8,81E-6	
0.00625	1.42E-5	2.14	1.27E-6	2.79
0.003125	3.31E-6	2.10	1.70E-7	2.91
0.0015625	7.97E-7	2.05	2.04E-8	3.06

Table 15: Accuracy of BFECC interpolation on perturbed and shifted grid in 3D.

is a test. After the rotation of a source grid with an angle, the results of BFECC interpolation are presented in Table 16. This test shows that the rotation has prevented the accuracy order of the BFECC interpolation from reaching 3rd order, but still the errors of BFECC interpolations is several times smaller than those of the underlying trilinear interpolation.

Rotation of 3° of a Rectangular grid				
	Trilinear		BFECC	
Δx	error	order	error	order
0.05	3.45E-3		1.51E-3	
0.025	7.48E-4	2.21	1.62E-4	3.22
0.0125	2.03E-4	1.88	3.56E-5	2.18
0.00625	4.61E-5	2.14	1.26E-5	1.50

Table 16: Accuracy of BFECC interpolation on rotated grid in 3D.

3 Application to Flow Problems

3.1 Corner Flow

A 3D corner flow was proposed to test accuracy of numerical schemes [19], and it is selected to test the performance of BFECC in simulation of flow problems. Consider a cubic box with length of 1.2 in each direction. Let u , v , and w be velocity in x , y , and z , respectively, and the origin of the coordinates are at the center of the cube). The fluid inside is initialized with zero speed, then an entrance velocity is imposed at the lid of the box as below:

$$w = -e^{1-2/t} \sin(\pi((x+0.5)^3 - 3(x+0.5)^2 + 3(x+0.5))(0.25 - y^2)) \quad (11)$$

It gradually drives the fluid to flow out at one of the lateral sides. The Reynolds number is $Re=100$, based on the edge length and the maximum velocity at the lid. The flow is simulated by solving the incompressible Navier-Stokes equations on overset grids together with trilinear interpolation at grid interfaces [16]. The Navier-Stokes equations are discretized by a 2nd order finite difference method in both time and space.

There are two overlapping cubes, the small cube ($0.8*0.8*0.8$) is placed inside the big cube ($1.2*1.2*1.2$). The edges of two cubes are parallel but the nodes are not coincided. Three sets of grids are used: 13^3 for the big cube and 9^3 for the small one as coarse grids, 25^3 and 17^3 as medium grids, and 49^3 and 33^3 as fine grids, see Fig.6. Additionally, a simulation is made used a single domain of 71^3 , and its solution is intended as a reference to be compared with.

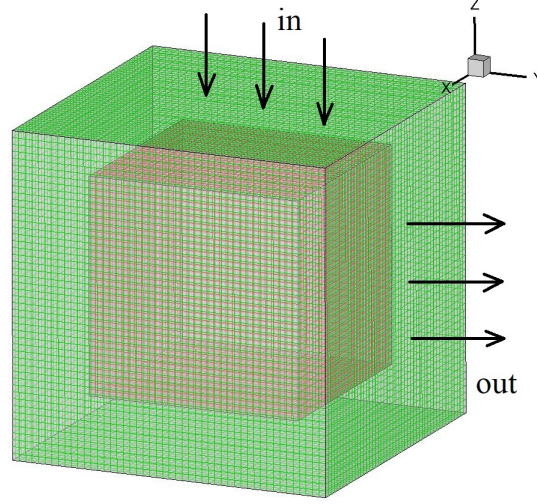


Figure 6: Fine mesh for the corner flow

Simulated instantaneous flow fields are shown in Fig. 7. It is seen that the solutions on the outer and inner cubes are identical at the scales of the figures. Further check on the solutions are made by looking at their accuracy orders with regard to time step and grid spacing. As stated in the Lax Theorem, in linear situations, an algorithm of pth -order leads to pth -order in accuracy order. In non-linear situation, such understanding is frequently true. In view that the algorithms to solve the flows inside cubes are 2^{nd} order accurate, and thus their convergence rates are expected to be 2^{nd} order. However, when the interface computation is treated by linear interpolation, which is 1^{st} order, the convergence rate will be around 1^{st} order. As a result, the overall accuracy order of solutions to the corner flows will be affected, or, degraded by the linear interpolation. As BFECC is applied at the interfaces, it is expected that the accuracy order will be recovered to 2^{nd} order.

With above understanding and also in view that there is no analytical solution for the flow, the accuracy order, κ , of the solutions are evaluated numerically by their values on three sets of grids listed above using the following formula (e.g., [19]):

$$\kappa = \log\left(\frac{\|f_{\Delta} - f_{\Delta/2}\|_2}{\|f_{\Delta/2} - f_{\Delta/4}\|_2}\right)/\log 2 \quad (12)$$

where f is solution for flow variables u , v , w , and p , and Δ , $\Delta/2$, and $\Delta/4$ stand for coarse, medium, and fine grids, respectively. It is noted that formula (12) is a rough estimate for the accuracy order and may not present its exact value.

The estimated solution accuracy order, κ , for the corner flow with the inner cube placed parallel to the outer one are plotted in Figs. 8, 9, and 10, with show the accuracy order at the interface, in

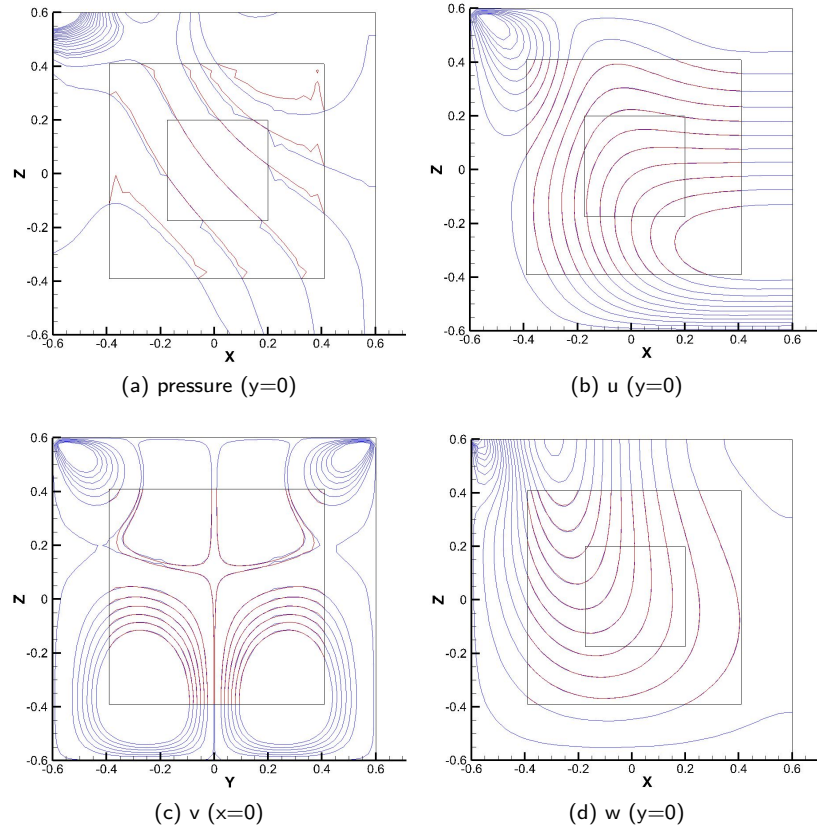


Figure 7: Contour line at $t=10$ s. The interfaces are treated by BFECC.

the inner cube, and in the outer cube, respectively. It is seen that the estimated accuracy orders are relatively low, and then after the flow develops for about 5-6 s, they become higher and stable. The low values at the initial time is attributed to that fact that the flow is highly transient and it is difficult for the formula (12) to capture the accuracy order. The figures show that in all parts of the flow field, the accuracy order of BFECC is a little higher than that by the interpolation, indicating that BFECC indeed enhances the accuracy of the interpolation and verifying the motion to apply BFECC at the interface. Interestingly, it is seen that MFBI also provides a better accuracy than the interpolation, primarily within the inner and outer cubes , although both of them are 1st order accurate.

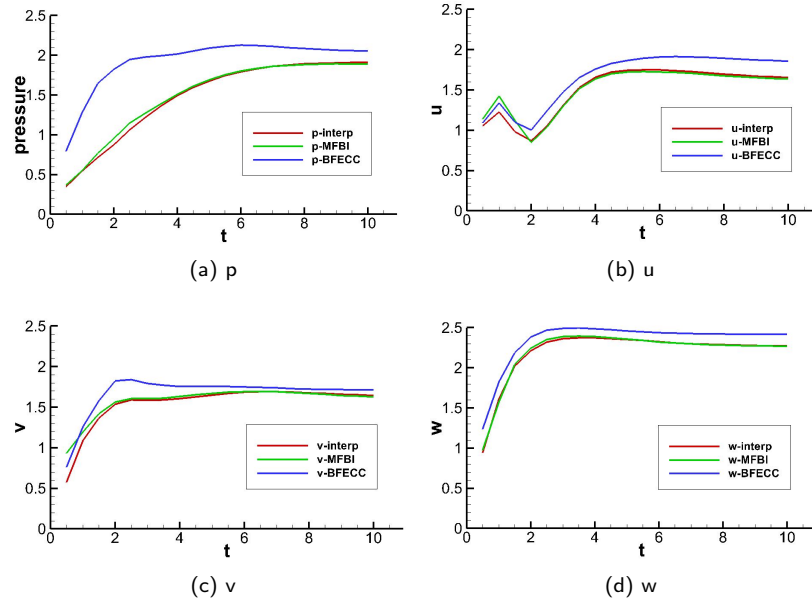


Figure 8: Accuracy order of corner flow at the interface, with inner cube parallel to the outer cube.

In order to get a better view on the accuracy of the three interface treatments, the average values of accuracy order over all time are summarized in Table.17, which clearly indicates statistically the order for better accuracy is BFECC, MFBI, and linear interpolation.

It is noted that, as indicated in above section, BFECC has certain restrictions in relative rotation of grids. In order to verify such understanding, another case of corner flow simulated with rotated inner cube has also been conducted. The result shows that still BFECC increases the accuracy of interpolation, although not as much as in the horizontal situation.

3.2 Cavity Flow

Cavity flow has been used to test numerical methods including interface algorithms [11, 16]. Within the cavity, the fluid is initially stationary, and it flows due to a gradual motion of the lid in the horizontal direction:

$$u = e^{-1/(5t)} + 0.01. \quad (13)$$

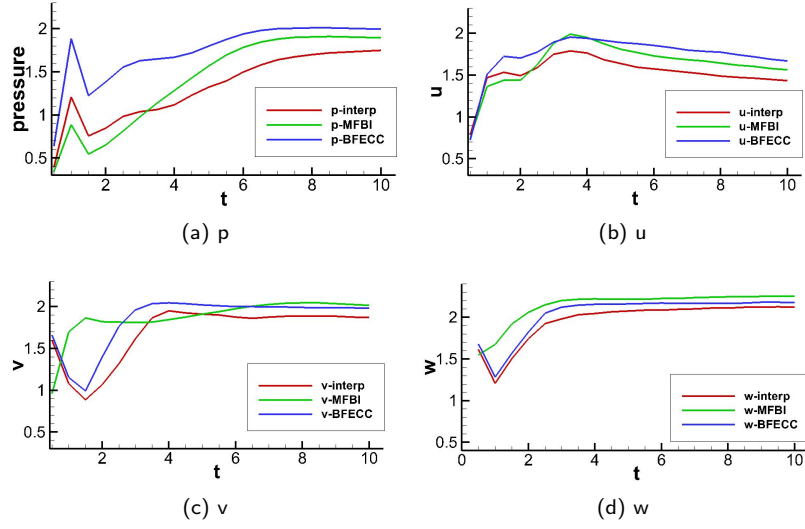


Figure 9: Accuracy order of corner flow in the inner cube, with inner cube parallel to the inner cube.

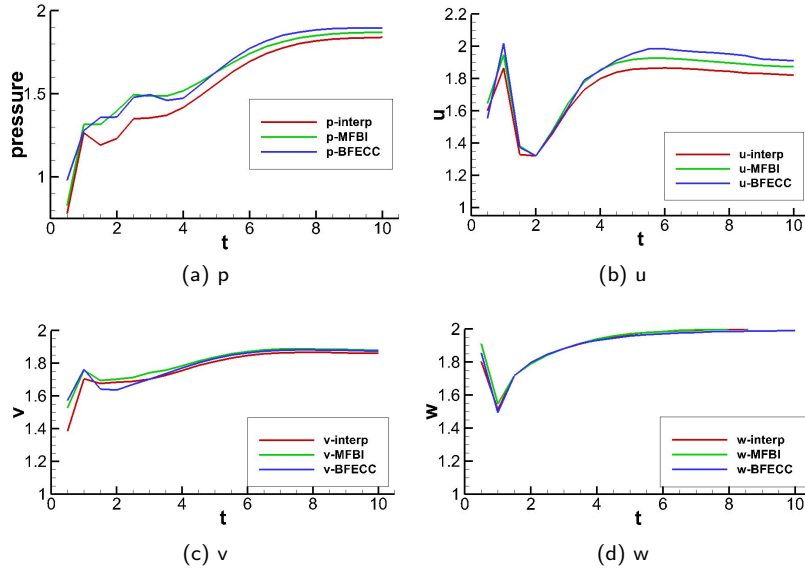


Figure 10: Accuracy order of corner flow in the outer cube, with inner cube parallel to the outer cube.

corner-hor		p	u	v	w	puvw
Interp	outer	1.54	1.74	1.78	1.91	1.74
	inner	1.32	1.53	1.70	1.96	1.63
	interface	1.48	1.51	1.55	2.20	1.68
MFBI	outer	1.61	1.79	1.81	1.92	1.78
	inner	1.41	1.63	1.88	2.14	1.77
	interface	1.49	1.52	1.58	2.20	1.70
BFECC	outer	1.63	1.82	1.79	1.91	1.79
	inner	1.75	1.74	1.85	2.04	1.85
	interface	1.93	1.66	1.67	2.34	1.90
'corner-hor': inner block placed parallel to outer block						

Table 17: Component convergence rate averaged over time for corner-hor.

As the flow is very complicated and it is difficult to estimate accuracy order of numerical solutions at high Reynolds numbers, we chose $Re=1$. In the computation, the flow domain is decomposed into two parts, upper part and lower part with an overlapping region in between, as shown in Fig.11. With origin of the coordinates at the center of the cavity, the upper part covers $(-0.5, 0.5) \times (-0.5, 0.5) \times (-0.12, 0.5)$, and the lower part occupies $(-0.5, 0.5) \times (-0.5, 0.5) \times (-0.5, 0.1)$. The interfaces of the two parts are at $z = -0.12$ and $z = 0.1$. Again, three sets of grids are used to estimate the convergence rate: 9^3 for the lower part and 11^3 for the upper part as coarse grids, 17^3 and 21^3 as medium grids, and 33^3 and 41^3 as fine grids. Also, a reference solution is achieved by employing a fine mesh of 61^3 .

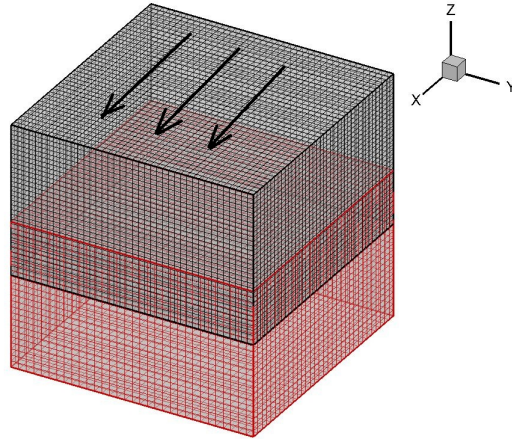


Figure 11: Meshes for transient cavity flow

The simulated flow fields are shown in Fig.12. As seen in the figure, the solutions in the lower and the upper parts are basically overlapping. To further analyze the results, similarly to discussion of the corner flow in above section, accuracy orders of the solutions are estimated and then plotted in Figs. 13, 14, and 15, which present the accuracy at the interface, in the lower part, and in the upper part. It is noted that the accuracy at the interface combines that at the two parts' interfaces, and the region

$0.2 < z < 0.5$ is excluded when estimating accuracy since the solutions at the upper left and right corners are singular. It is seen in these figures that the estimated accuracy is low at the first a few seconds, and later it reaches a stable value around 2nd order. The result indicates that BFECC indeed enhances the accuracy of the numerical solution.

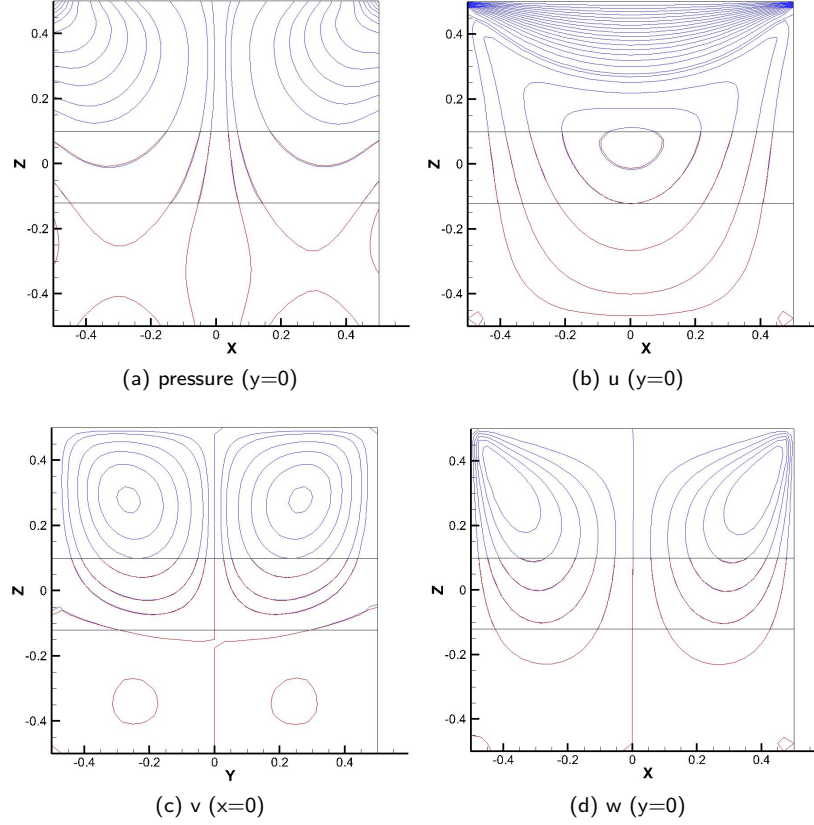


Figure 12: Solutions of cavity flow obtained with BFECC, at $t=1.0s$

The average values of accuracy order over all time are summarized in Table.18, which shows statistically the order for better accuracy is BFECC, MFBI, and linear interpolation.

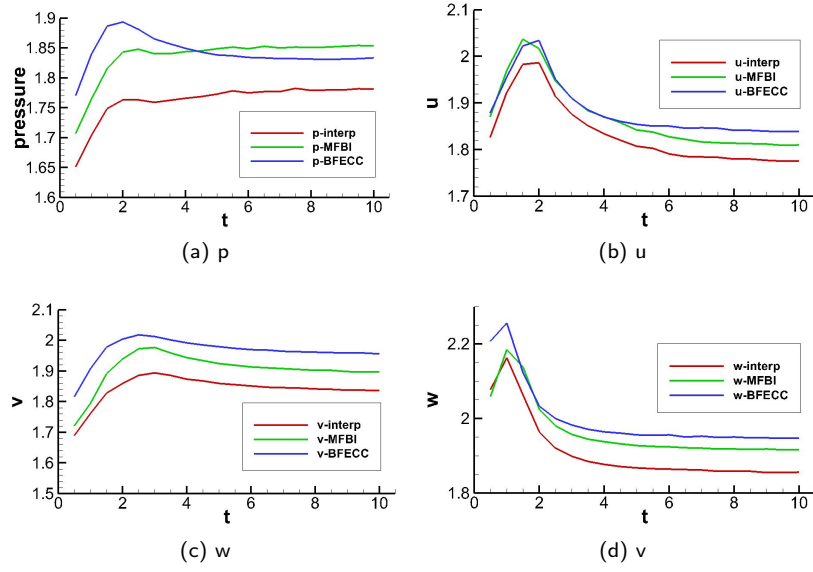


Figure 13: Accuracy order of cavity flow at the interface.

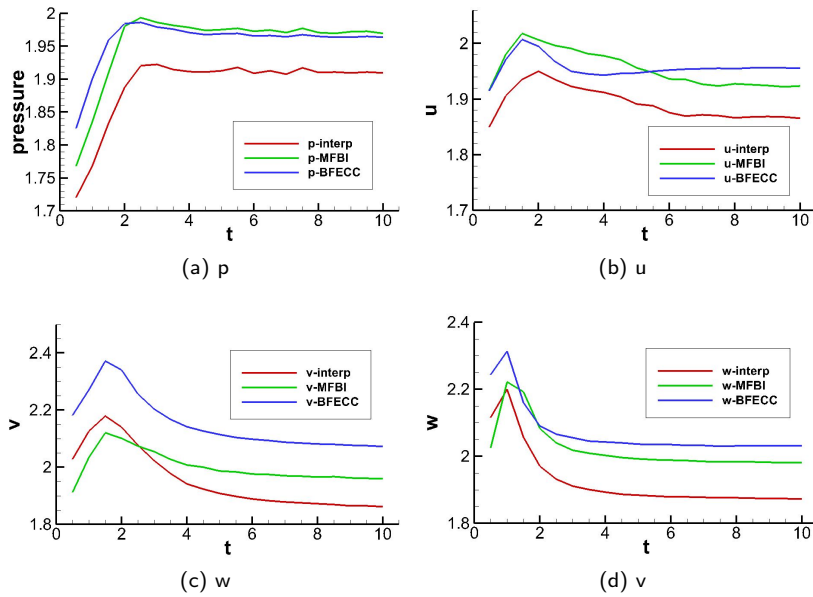


Figure 14: Accuracy order of cavity flow in the lower part.

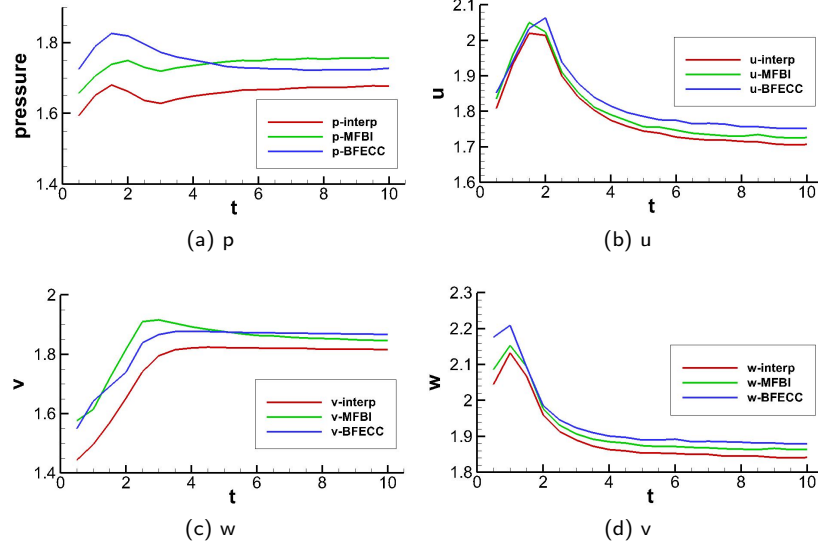


Figure 15: Accuracy order of cavity flow in the upper part.

cavity		p	u	v	w	puvw
Interp	upper	1.66	1.79	1.76	1.90	1.78
	lower	1.89	1.89	1.95	1.93	1.92
	interface	1.76	1.83	1.84	1.91	1.84
MFBI	upper	1.74	1.81	1.83	1.92	1.82
	lower	1.96	1.95	2.00	2.02	1.98
	interface	1.84	1.87	1.91	1.96	1.89
BFECC	upper	1.75	1.83	1.83	1.94	1.84
	lower	1.96	1.96	2.15	2.07	2.03
	interface	1.84	1.88	1.97	1.99	1.92

Table 18: Component convergence rate averaged over time for cavity

4 Conclusion

BFECC interpolation is able to improve the order of accuracy of the underlying linear interpolation method by one when interpolating from a rectangular grid to its translation, even if a smooth perturbation is applied to the translation. If the translated grid points are located at centroids of the original grid, then BFECC interpolation (based on linear interpolation) is able to reach fourth order accuracy, a “super-convergence” phenomenon. These properties could be useful in high dimensional data and will be studied in the future. When interpolating from a rectangular grid to its rotation, BFECC interpolation will not improve the order of the underlying linear interpolation, but will usually reduce the size of the linear interpolation error.

The investigation here is based on structured meshes. But the BFECC method also works on triangle meshes [13, 14]. In the next step, it is planned to apply this method to the coupled modeling system ‘SIFOM-FVCOM’ [18] (SIFOM is a solver for the Navier-Stokes equations, and FVCOM is a solver for the geophysical fluid dynamics equations). But a new treatment is needed as the two coupled models use different types of meshes (structured mesh for SIFOM and unstructured mesh for FVCOM).

References

- [1] I. Llamas B.-M. Kim, Y.-J. Liu and J. Rossignac. FlowFixer: Using BFECC for fluid simulation. *Eurographics Workshop on Natural Phenomena*, 2005.
- [2] I. Llamas B.-M. Kim, Y.-J. Liu and J. Rossignac. Advections with significantly reduced dissipation and diffusion. *IEEE Transactions on Visualization and Computer Graphics*, 13:135–144, 2007.
- [3] T. Barth and P. Frederickson. Higher order solution of the euler equations on unstructured grids using quadratic reconstruction. *28th Aerospace Sciences Meeting*, page 13, 1990.
- [4] J. A. Benek, J. L. Steger, and F. C. Dougherty. A flexible grid embedding technique with application to the Euler equations. Technical report, AIAA, 1983.
- [5] Y. Chen, Q.-J. Kang, Q.-D. Cai, and D.-X. Zhang. Lattice boltzmann method on quadtree grids. *Physical Review E*, 83:1–10, 2011.
- [6] G. Chesshire and W. D. Henshaw. Composite overlapping meshes for the solution of partial differential equations. *J. Comput. Phys.*, 90:1–64, 1990.
- [7] R. Courant, E. Isaacson, and M. Rees. On the solution of nonlinear hyperbolic differential equations by finite differences. *Comm. Pure Appl. Math.*, 5:243–255, 1952.
- [8] T. F. Dupont and Y.-J. Liu. Back and forth error compensation and correction methods for removing errors induced by uneven gradients of the level set function. *J. Comput. Phys.*, 191:311–324, 2003.
- [9] T. F. Dupont and Y.-J. Liu. Back and forth error compensation and correction methods for semi-lagrangian schemes with application to level set interface computations. *Math. Comp.*, 76:647–668, 2007.
- [10] J. F. Epperson. *An Introduction to Numerical Methods and Analysis*, 2nd edition. Wiley, 2013.
- [11] K. Goda. Multistep technique with implicit difference schemes for calculating 2-dimensional or 3-dimensional cavity flows. *J. Comput. Phys.*, 30:76–95, 1979.
- [12] C. Hu and C.-W. Shu. Weighted essentially non-oscillatory schemes on triangular meshes. *J. Comput. Phys.*, 150:97–127, 1999.
- [13] L.-L. Hu. Numerical algorithms based on the back and forth error compensation and correction. *PhD thesis, Georgia Inst. of Tech.*, 2014.
- [14] L.-L. Hu, Y. Li, and Y.-J. Liu. A limiting strategy for the back and forth error compensation and correction method for solving advection equations. *Math. Comput.*, 85:1263–1280, 2016.

- [15] A. Selle, R. Fedkiw, B.-M. Kim, Y.-J. Liu, and J. Rossignac. An unconditionally stable maccormack method. *J. Sci. Comput.*, 35:350–371, 2008.
- [16] H.-S. Tang. Study on a grid interface algorithm for solutions of incompressible navier-stokes equations. *Computers & Fluids*, 35:1372–1383, 2006.
- [17] H. S. Tang, C. Jones, and F. Sotiropoulos. An overset grid method for 3D unsteady incompressible flows. *J. Comput. Phys.*, 191:567–600, 2003.
- [18] H.-S. Tang, K. Qu, and X.-G. Wu. An overset grid method for integration of fully 3D fluid dynamics and geophysical fluid dynamics models to simulate multiphysics coastal ocean flows. *J. Comput. Phys.*, 273:548–571, 2014.
- [19] H.-S. Tang and F. Sotiropoulos. Fractional step artificial compressibility method for navier-stokes equations. *Computers & Fluids*, 36:974–986, 2007.
- [20] H. S. Tang and T. Zhou. On nonconservative algorithms for grid interfaces. *SIAM J. Numer. Anal.*, 37:173–193, 1999.
- [21] H.-Z. Tang and T. Tang. Adaptive mesh methods for one-and two-dimensional hyperbolic conservation laws. *SIAM Journal on Numerical Analysis*, 41:487–515, 2003.
- [22] K. M. Terekhov, K. D. Nikitin, M. A. Olshanskii, and Y. V. Vassilevski. A semi-lagrangian method on dynamically adapted octree meshes. *Russ. J. Numer. Anal. Math. Modelling*, 30:363–380, 2015.
- [23] X. Wang and Y. Liu. Back and forth error compensation and correction method for linear hyperbolic systems with application to the Maxwell's equations. *Journal of Computational Physics: X*, 1:100014, 2019.

Appendices

All works in the appendices are conducted using 'Mathematica', version: 11.3.0.

A BFECC interpolation in 1D based on linear interpolation is 3rd order accurate

This part is derived in a 1D situation. The grid spacing in each domain is assumed to be the same ($dx_1=dx_2$). 'g' is the source domain and 'f' is the target domain. The code is attached below:

1. Taylor series:

```
gin1= f-(1+a)*fx+(1+a)^2*fx/2-(1+a)^3*fx/6+(1+a)^4*fx/24
gi = f-a*fx +a^2*fx/2 -a^3*fx/6 +a^4*fx/24
gip1= f+(1-a)*fx+(1-a)^2*fx/2+(1-a)^3*fx/6+(1-a)^4*fx/24
gip2= f+(2-a)*fx+(2-a)^2*fx/2+(2-a)^3*fx/6+(2-a)^4*fx/24
```

2. BFECC procedure:

```
fin1= a*gi + (1-a)*gin1
fi = a*gip1 + (1-a)*gi
fip1= a*gip2 + (1-a)*gip1

ggi = a*fin1 + (1-a)*fi
ggip1= a*fi + (1-a)*fip1

ggi = gi + (gi-ggi)/2
ggip1= gip1 + (gip1-ggip1)/2

ffi = a*ggip1 + (1-a)*ggi
```

The BFECC interpolation result:

$$ffi = f + \frac{a(a-1)[(8a-4)fx - 9a(a-1)fx^3]}{24}$$

3. The linear interpolation result:

$$fi = f + \frac{a(1-a)[12fx + (4-8a)fx^3 + (1-3a+3a^2)fx^3]}{24}$$

B BFECC interpolation in 2D based on bilinear interpolation is 3rd order accurate

This part is derived in a 2D situation. The grid spacing in each domain is assumed to be the same ($dx1=dx2$, $dy1=dy2$, but $dx1 \neq dy1$ & $dx2 \neq dy2$). 'g' is the source domain and 'f' is the target domain. The code is attached below:

1. Taylor series:

$$\begin{aligned}
 g1 &= f - (1+b)*x*fx - (1+a)*y*fy + (1+b)^2*x^2*fxx/2 + (1+a)^2*y^2*fyy/2 \\
 &\quad + (1+a)*(1+b)*x*y*fxy - (1+b)^3*x^3*fxxx/6 - (1+a)^3*y^3*fyyy/6 \\
 &\quad - (1+b)^2*(1+a)*x^2*y*fxy/2 - (1+b)*(1+a)^2*x*y^2*fxy/2 \\
 g2 &= f - b*x*fx - (1+a)*y*fy + b^2*x^2*fxx/2 + (1+a)^2*y^2*fyy/2 \\
 &\quad + (1+a)*b*x*y*fxy - b^3*x^3*fxxx/6 - (1+a)^3*y^3*fyyy/6 \\
 &\quad - b^2*(1+a)*x^2*y*fxy/2 - b*(1+a)^2*x*y^2*fxy/2 \\
 g3 &= f + (1-b)*x*fx - (1+a)*y*fy + (1-b)^2*x^2*fxx/2 + (1+a)^2*y^2*fyy/2 \\
 &\quad - (1+a)*(1-b)*x*y*fxy + (1-b)^3*x^3*fxxx/6 - (1+a)^3*y^3*fyyy/6 \\
 &\quad - (1-b)^2*(1+a)*x^2*y*fxy/2 + (1-b)*(1+a)^2*x*y^2*fxy/2 \\
 g4 &= f + (2-b)*x*fx - (1+a)*y*fy + (2-b)^2*x^2*fxx/2 + (1+a)^2*y^2*fyy/2 \\
 &\quad - (1+a)*(2-b)*x*y*fxy + (2-b)^3*x^3*fxxx/6 - (1+a)^3*y^3*fyyy/6 \\
 &\quad - (2-b)^2*(1+a)*x^2*y*fxy/2 + (2-b)*(1+a)^2*x*y^2*fxy/2 \\
 g5 &= f - (1+b)*x*fx - a*y*fy + (1+b)^2*x^2*fxx/2 + a^2*y^2*fyy/2 \\
 &\quad + a*(1+b)*x*y*fxy - (1+b)^3*x^3*fxxx/6 - a^3*y^3*fyyy/6 \\
 &\quad - (1+b)^2*a*x^2*y*fxy/2 - (1+b)*a^2*x*y^2*fxy/2 \\
 g6 &= f - b*x*fx - a*y*fy + x^2*b^2*fxx/2 + y^2*a^2*fyy/2 \\
 &\quad + x*y*a*b*fxy - x^3*b^3*fxxx/6 - y^3*a^3*fyyy/6 \\
 &\quad - x^2*y*b^2*a*fxy/2 - x*y^2*b*a^2*fxy/2 \\
 g7 &= f + (1-b)*x*fx - a*y*fy + (1-b)^2*x^2*fxx/2 + a^2*y^2*fyy/2 \\
 &\quad - (1-b)*a*x*y*fxy + (1-b)^3*x^3*fxxx/6 - a^3*y^3*fyyy/6 \\
 &\quad - (1-b)^2*a*x^2*y*fxy/2 + (1-b)*a^2*x*y^2*fxy/2 \\
 g8 &= f + (2-b)*x*fx - a*y*fy + (2-b)^2*x^2*fxx/2 + a^2*y^2*fyy/2 \\
 &\quad - (2-b)*a*x*y*fxy + (2-b)^3*x^3*fxxx/6 - a^3*y^3*fyyy/6 \\
 &\quad - (2-b)^2*a*x^2*y*fxy/2 + (2-b)*a^2*x*y^2*fxy/2 \\
 g9 &= f - (1+b)*x*fx + (1-a)*y*fy + (1+b)^2*x^2*fxx/2 + (1-a)^2*y^2*fyy/2 \\
 &\quad - (1-a)*(1+b)*x*y*fxy - (1+b)^3*x^3*fxxx/6 + (1-a)^3*y^3*fyyy/6 \\
 &\quad + (1+b)^2*(1-a)*x^2*y*fxy/2 - (1+b)*(1-a)^2*x*y^2*fxy/2 \\
 g10 &= f - b*x*fx + (1-a)*y*fy + b^2*x^2*fxx/2 + (1-a)^2*y^2*fyy/2 \\
 &\quad - b*(1-a)*x*y*fxy - b^3*x^3*fxxx/6 + (1-a)^3*y^3*fyyy/6 \\
 &\quad + b^2*(1-a)*x^2*y*fxy/2 - b*(1-a)^2*x*y^2*fxy/2 \\
 g11 &= f + (1-b)*x*fx + (1-a)*y*fy + (1-b)^2*x^2*fxx/2 + (1-a)^2*y^2*fyy/2 \\
 &\quad + (1-a)*(1-b)*x*y*fxy + (1-b)^3*x^3*fxxx/6 + (1-a)^3*y^3*fyyy/6 \\
 &\quad + (1-b)^2*(1-a)*x^2*y*fxy/2 + (1-b)*(1-a)^2*x*y^2*fxy/2 \\
 g12 &= f + (2-b)*x*fx + (1-a)*y*fy + (2-b)^2*x^2*fxx/2 + (1-a)^2*y^2*fyy/2 \\
 &\quad + (1-a)*(2-b)*x*y*fxy + (2-b)^3*x^3*fxxx/6 + (1-a)^3*y^3*fyyy/6 \\
 &\quad + (2-b)^2*(1-a)*x^2*y*fxy/2 + (2-b)*(1-a)^2*x*y^2*fxy/2 \\
 g13 &= f - (1+b)*x*fx + (2-a)*y*fy + (1+b)^2*x^2*fxx/2 + (2-a)^2*y^2*fyy/2 \\
 &\quad - (2-a)*(1+b)*x*y*fxy - (1+b)^3*x^3*fxxx/6 + (2-a)^3*y^3*fyyy/6
 \end{aligned}$$

$$\begin{aligned}
& + (1+b)^2(2-a)x^2y f_{xxy}/2 - (1+b)(2-a)^2xy^2 f_{xyy}/2 \\
g14 = & f - bxxfx + (2-a)yfy + b^2x^2 f_{xx}/2 + (2-a)^2y^2 f_{yy}/2 \\
& - (2-a)bxy f_{xy} - b^3x^3 f_{xxx}/6 + (2-a)^3y^3 f_{yyy}/6 \\
& + b^2(2-a)x^2y f_{xxy}/2 - b(2-a)^2xy^2 f_{xyy}/2 \\
g15 = & f + (1-b)xxfx + (2-a)yfy + (1-b)^2x^2 f_{xx}/2 + (2-a)^2y^2 f_{yy}/2 \\
& + (2-a)(1-b)xy f_{xy} + (1-b)^3x^3 f_{xxx}/6 + (2-a)^3y^3 f_{yyy}/6 \\
& + (1-b)^2(2-a)x^2y f_{xxy}/2 + (1-b)(2-a)^2xy^2 f_{xyy}/2 \\
g16 = & f + (2-b)xxfx + (2-a)yfy + (2-b)^2x^2 f_{xx}/2 + (2-a)^2y^2 f_{yy}/2 \\
& + (2-a)(2-b)xy f_{xy} + (2-b)^3x^3 f_{xxx}/6 + (2-a)^3y^3 f_{yyy}/6 \\
& + (2-b)^2(2-a)x^2y f_{xxy}/2 + (2-b)(2-a)^2xy^2 f_{xyy}/2
\end{aligned}$$

2. BFECC procedure:

$$\begin{aligned}
f1 = & (g1 * (1-a) + g5 * a) * (1-b) + (g2 * (1-a) + g6 * a) * b \\
f2 = & (g2 * (1-a) + g6 * a) * (1-b) + (g3 * (1-a) + g7 * a) * b \\
f3 = & (g3 * (1-a) + g7 * a) * (1-b) + (g4 * (1-a) + g8 * a) * b \\
f4 = & (g5 * (1-a) + g9 * a) * (1-b) + (g6 * (1-a) + g10 * a) * b \\
f5 = & (g6 * (1-a) + g10 * a) * (1-b) + (g7 * (1-a) + g11 * a) * b \\
f6 = & (g7 * (1-a) + g11 * a) * (1-b) + (g8 * (1-a) + g12 * a) * b \\
f7 = & (g9 * (1-a) + g13 * a) * (1-b) + (g10 * (1-a) + g14 * a) * b \\
f8 = & (g10 * (1-a) + g14 * a) * (1-b) + (g11 * (1-a) + g15 * a) * b \\
f9 = & (g11 * (1-a) + g15 * a) * (1-b) + (g12 * (1-a) + g16 * a) * b
\end{aligned}$$

$$\begin{aligned}
gg6 = & (f1 * a + f4 * (1-a)) * b + (f2 * a + f5 * (1-a)) * (1-b) \\
gg7 = & (f2 * a + f5 * (1-a)) * b + (f3 * a + f6 * (1-a)) * (1-b) \\
gg10 = & (f4 * a + f7 * (1-a)) * b + (f5 * a + f8 * (1-a)) * (1-b) \\
gg11 = & (f5 * a + f8 * (1-a)) * b + (f6 * a + f9 * (1-a)) * (1-b)
\end{aligned}$$

$$\begin{aligned}
ggg6 = & g6 + 0.5 * (g6 - gg6) \\
ggg7 = & g7 + 0.5 * (g7 - gg7) \\
ggg10 = & g10 + 0.5 * (g10 - gg10) \\
ggg11 = & g11 + 0.5 * (g11 - gg11)
\end{aligned}$$

$$ff5 = (ggg6 * (1-a) + ggg10 * a) * (1-b) + (ggg7 * (1-a) + ggg11 * a) * b$$

The BFECC interpolation result:

$$ffi = f + \frac{(b - 3b^2 + 2b^3)dx^3 * f_{xxx} + (a - 3a^2 + 2a^3)dy^3 * f_{yyy}}{6}$$

3. The bilinear interpolation result:

$$\begin{aligned}
fi = & f + \frac{(3b - 3b^2)dx^2 * f_{xx} + (b - 3b^2 + 2b^3)dx^3 * f_{xxx}}{6} \\
& + \frac{3a(1-a)dy^2 * f_{yy} + a(2a-1)(a-1)dy^3 * f_{yyy}}{6}
\end{aligned}$$

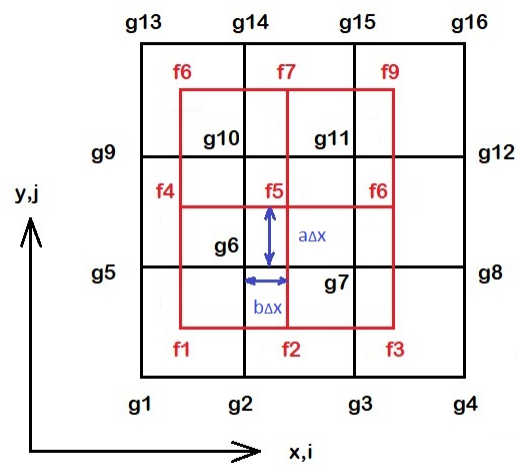


Figure 16: Interpolation coefficients and node index